The Steepbank crosswell seismic project: Reservoir definition and evaluation of steamflood technology in Alberta tar sands

By B.N.P. PAULSSON, J.A. MEREDITH, Z. WANG
Chevron Petroleum Technology Co.
La Habra, California

and J. W. FAIRBORN
Well Seismic Computing Services
Newport Beach, California

Two crosswell seismic surveys were conducted at Chevron Canada's Oil Sand Lease 49 (Steepbank) located about 60 km northeast of Fort McMurray, Alberta. This is the site of the HASDrive commercial pilot project in which steam is circulated through a horizontal well in order to preheat the tar sand prior to conventional steam injection. The objective of the crosswell survey was to define the geology and to monitor the movement of the injected steam as part of the HASDrive evaluation. The first survey was conducted 25 September-6 October 1991, just prior to steam injection. The second was acquired 7-14 January 1992, after 72 days of continuous steam injection.

It is well known that seismic velocities decrease with increased temperature in heavy oil, unconsolidated sand, or sandstone reservoirs. Thus any velocity reduction between the surveys would indicate the distribution of increased temperature and, by inference, the flow path the steam had taken.

The surveys were successful in monitoring steam injection. We could, however, not find a simple relationship between velocity and porosity that would have taken us one step further to create a flow model for reservoir characterization. On the other hand, the data are of very high quality and complexity and, as an example of a dataset collected in a difficult operational and geologic environment, it has been invaluable.

HASDrive process. This acronym stands for Heated Annulus Steam Drive. The process circulates steam through the annulus of a horizontal well in order to heat a zone of the reservoir surrounding the well. The steam is not injected into the formation; it is circulated through the well and heating is by conduction. The heat reduces the viscosity of the bitumen, allowing it to mobilize under conventional steam drive. On the other hand, steam injected into cold bitumen forms an impermeable tar bank as the bitumen concentrates. Consequently, steam injected into the formation by a conventional vertical injector sweeps the preheated zone of mobilized bitumen and is blocked elsewhere by the tar bank.

Figure 1 shows a map view of the pilot site and a cross section through the center of the site. There are two steam injectors with the producing well in between. Only the first injection well, IN1, is shown in Figure 1. The production well and the other injection well are located southeast (off the right end of the figure) at distances of 119 and 250 m from IN1,

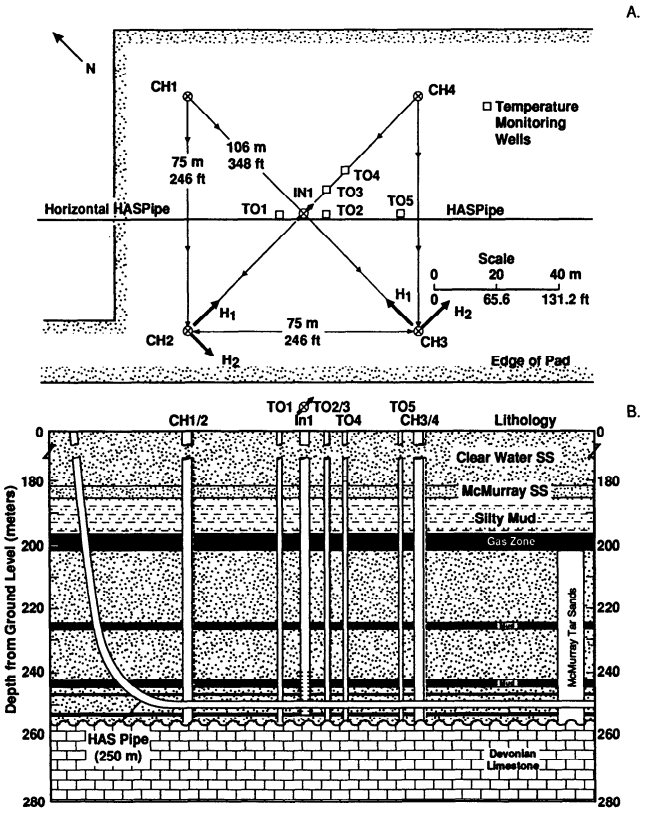

Figure 1. Site plan and cross section of HASDrive pilot project showing the horizontal well and injection well IN1. Wells TO1-TO5 are for temperature observations. Chl-Ch4 are crosswell survey wells. Geologic model in the background.

respectively. All were drilled as close to the horizontal well as possible to ensure that steam injection and oil production were within the preheated zone. Wells TOl-TO5 were drilled for temperature observations.

Field procedures. The crosshole survey wells, Chl-Ch4, are also shown in Figure 1. They are located at the corners of a square., 75 m on a side and centered on injection well IN1. Ch1 and Ch4 were the source wells, Ch2 and Ch3 the receiver wells. Recording each shot into bath receiver wells resulted in four tomography sections, two intersecting IN1 along the diagonals of the square and two along its northwest and southeast edges. Source and receiver depth intervals were 2.0 m. There were a total of 80 source and receiver levels, ranging from 160 to 3 18 m below ground. The seismic source was the vertical, borehole-clamped, hydraulic vibrator developed at Chevron (Figure 2). It is analogous to surface vibroseis; the clamp acts as the baseplate and "drive" comes from a vertically vibrating reaction mass suspended below the clamp. The hydraulic pump and motor are at the surface; hydraulic fluid is fed to the actuator through hoses which, along with an electrical cable, are clamped to the wireline. This tedious procedure will be replaced by the next generation borehole vibrator, currently being developed by a consortium (including several oil companies, Sandia National Laboratories, and GRI) in which all components will be inside the sonde. Due to the power requirements of the new source, it will be operated on a special heavy duty wireline.

Two 80-level, three-component geophone arrays were cemented into Ch2 and Ch3. The arrays were clamped to the outside of the tubing and lowered down through the casing. Cement was pumped through the tubing and around the geophones in the annulus between tubing and casing. Displacing the cement inside the tubing allowed the receiver wells to remain available for temperature observations and other wireline surveys. Geophones were carefully oriented so one horizontal component pointed along the diagonal of the square in the direction of the injection well (Figures 1, 13). Depth of each geophone was verified by placing a radioactive cobalt marker on the three-component geophone pod which could, after deployment, be detected by a gamma my survey. Deployment went smoothly. Pod depths were verified and particle motion plots of incident P-waves indicated that geophones were within five degrees of their intended orientation.

The 80-level arrays provided two important benefits. They increased the rate of data acquisition since, in principle, an entire shot fan could be recorded in one shot. Almost as important was the improvement in data quality. The cement provided perfect coupling to the formation. Tube wavenoise, a universal problem for liquid-filled borehole measurements, was nonexistent; the response of the vertical and horizontal components, usually quite different with mechanically clamped geophones, was nearly identical. Using these higher quality receiver arrays also resulted in significant cost savings. The cost of manufacturing and deploying the arrays was about $100 000. Typical recording costs for a crosswell survey are about $10 000 per day, so the arrays become cost effective after saving 10 days of survey time. We estimate the arrays saved at least 20 days of recording time, and probably more since additional time would also have increased chances of equipment failure.

Data acquisition included a 15-s linear sweep between 10 and 640 Hz. Sample interval was 0.5 ms. Two sweeps per depth position were sufficient for good signal-to-noise ratio. Data processing started in the field, which proved invaluable for quality control and for getting a jump start on the tomography inversion. In the second survey, we were able to compute a preliminary tomogram about 24 hours after recording.

Steepbank geology. Figure 1 shows the principal stratigraphic units at Steepbank. The geologic model was developed using log information from all the wells at the site. The formations are almost flat lying, although the top of the Paleozoic carbonate is karsted and irregular. The McMurray tar sand is a massive, unconsolidated sand with some mud stringers which appear to play a role in steam migration. A low velocity gas cap is at the top of the McMurray. We tried to establish relationships between sonic log velocities and

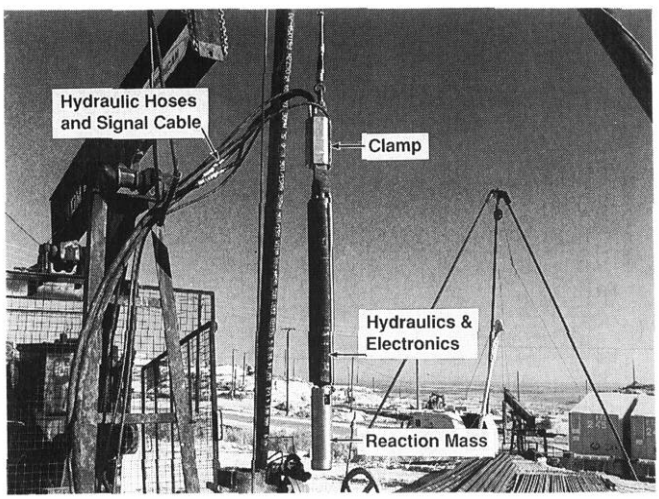

Figure 2. Downhole hydraulic vibrator.

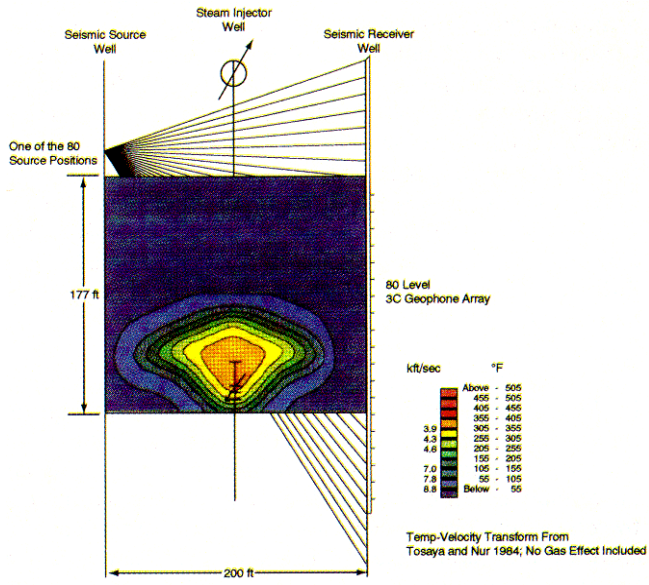

Figure 3. Results of thermal modeling at the vertical steam injector through a section perpendicular to HASPipe. The simplified geologic model results in a well behaved radially symmetric steam distribution near the injector.

variables needed for reservoir characterization, such as permeability and bitumen saturation, but were unable to find a consistent trend.

The gas cap and the carbonate interface at the base of the McMurray produce strong velocity contrasts. Both greatly complicate the seismic data, since. they cause strong refractions, reverberations, head waves, mode conversions, and scattering. This, in turn, makes interpretation difficult despite good data quality. The more important effect, however, is that the strong refractions lead to irregular ray paths so that portions of the tomography section could have sparse ray coverage.

The HASDRive horizontal well (the HAsPipe) is at a depth of about 250 m, just above the base of the McMurray tar sand. Figure 3 shows temperature contours surrounding HASPipe, computed from a flow simulator after 50 days of heating and steam injection. The calculations used the model shown in Figure 1, although the thin mudstone layers within the McMurray were not included.

Data examples. Figure 4 shows the three components of motion for the 158-m, common shot fan from section Ch4-Ch3. They are a good example of uncomplicated direct arrivals. Here the horizontal components are 4.5 degrees to the source well direction. Detailed analysis shows the amplitude and phase of the two horizontal components arc very similar, as they should be. Many coherent events are apparent after the first arrival. Crosswell reflections can be seen emerging from the first breaks with opposite moveout. For example, the reflection originating at about 268 m is from the top of the carbonate, the reflection at about 202 is from the gas cap. The low velocity gas cap is also responsible for the sharp time delay in the direct arrival pattern at 200 m. The event peeling away from the direct arrival at about 202 m, in the same direction but at greater moveout, is a converted, transmitted shear wave--another product of the gas cap.

Recording with geophones rather than hydrophones adds the complication of directivity pattern to the data. On the other hand, this can help in identifying the nature of the tint arrival. The axial vibrator is a dipole source in which the polarity of the upper P-wave lobe is opposite to that of the lower. In a homogeneous medium, therefore, the vertical component of the direct *P-wave* will be the same on all receivers, whereas the polarity of the horizontal component will reverse at the shot depth. In heterogeneous media, on the other hand, rays are refracted and, as shown in the top part of

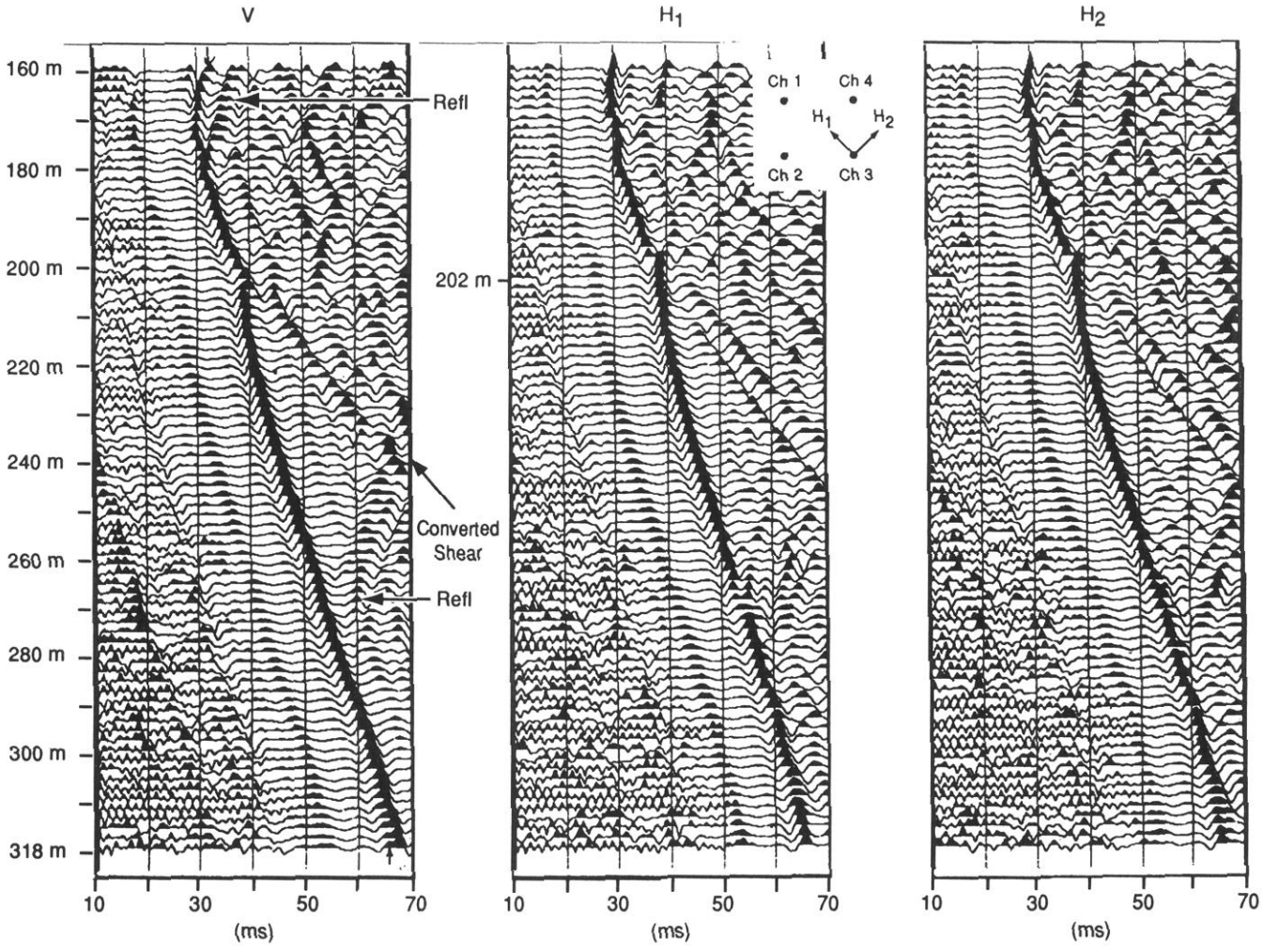

Figure 4. Common source fan fmm section Ch4-Ch3 at source depth of 160 m. Low amplitude zone before first arrival due to the 15 ms AGC operator. Note reflections at depths 176,202, and 268 m, and transmitted P-S converted wave at 204 m.

Figure 5, they can actually turn around if the velocity gradient is high enough. When this happens, the polarity of the vertical component will be reversed, but the horizontal component will not. Consequently, a polarity reversal seen on the vertical component but not on the horizontal indicates a turning ray, while a polarity reversal on the horizontal component but not on the vertical indicates the nodal point on the P-wave directivity pattern.

The common shot gather shown in the lower portion of Figure 5 is from section Ch4-Ch2. It displays a complicated pattern of events. The shot depth is 240 m which is just above the noisy vertical trace near the middle of the fan. Note that the fastest ray does not go through the receiver at 240 m, the one closest to the shot. Instead the traveltime decreases below receiver depth 240 m and reaches a minimum at about 276 m. This traveltime pattern is due to first arrivals having dipped down into the high velocity carbonate rather than going straight through the McMurray. As can be inferred from the polarity, as described above, all first arrivals between receiver depths 220-270 m represent waves that departed from the source in a downward direction, turned around inside a high velocity gradient, and intersected receivers traveling upward.

In fact, the wavefront that has turned around inside the carbonate continues upward as thesecond event on receivers above 220 m. Above that depth, the first arrival becomes the direct wave traveling entirely through the McMurray.

The late arriving event on Figure 5 is the shear wave, which appears as a very high amplitude event on all traces above the carbonate. Below the carbonate, however, things get complicated. The large velocity contrasts give rise to reverberation and S-to-P mode conversions. These complications make it difficult to pick the traveltime below 260 m and. consequently, the shear wave tomograms are. of poor quality.

The effect of the steam on the P-wave traveltime is shown in Figure 6, which is an overlay of traces from survey 1 and survey 2 as recorded on the 240-m common shot fan for Ch4-Ch2. Close examination shows the traces separate above about 240 m. Below 240 m the traces appear identical, verifying the repeatability of the two surveys and indicating that steam injection has added little heat below 240 m. Traveltime differences between the surveys are small, but still easily detected, and they drive the tomographic velocity differences discussed in a later section.

Data processing and tomography computation. Data processing was straightforward. Basically it consisted of format conversion, geometry assignment, a few single-trace processes for signal enhancement such as AGC and filter, and traveltime picking.

(We experimented with three-component coordinate rota-

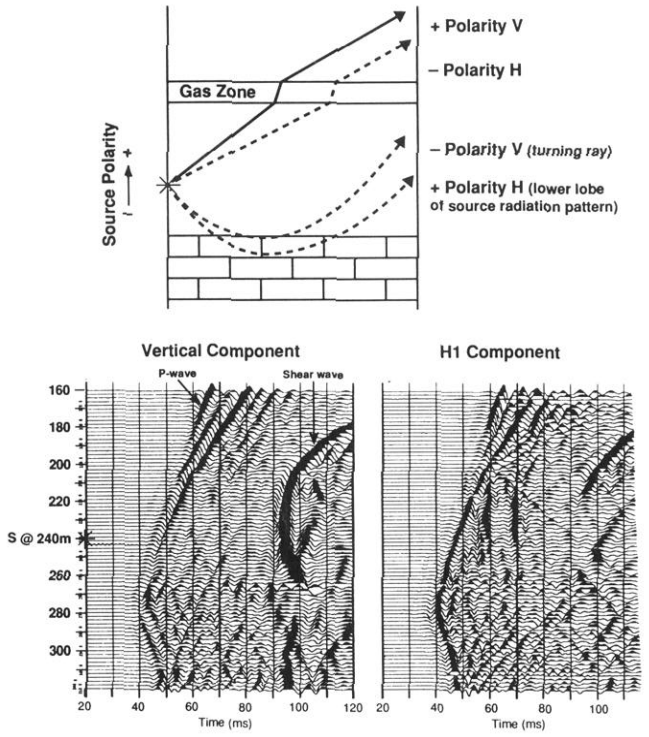

Figure 5. Common source fan from section Ch4-Ch2 at source depth of 240 m. Traveltimes continue to decrease below the closest receiver depth of 240 m because the fastest rays we turning around in the underlying carbonate. Turning rays are the first arrivals up to a depth of 220 m. Upper portion shows how the polarity of turning rays is reversed at the nodal point of the P-wave radiation pattern from the downhole vibrator.

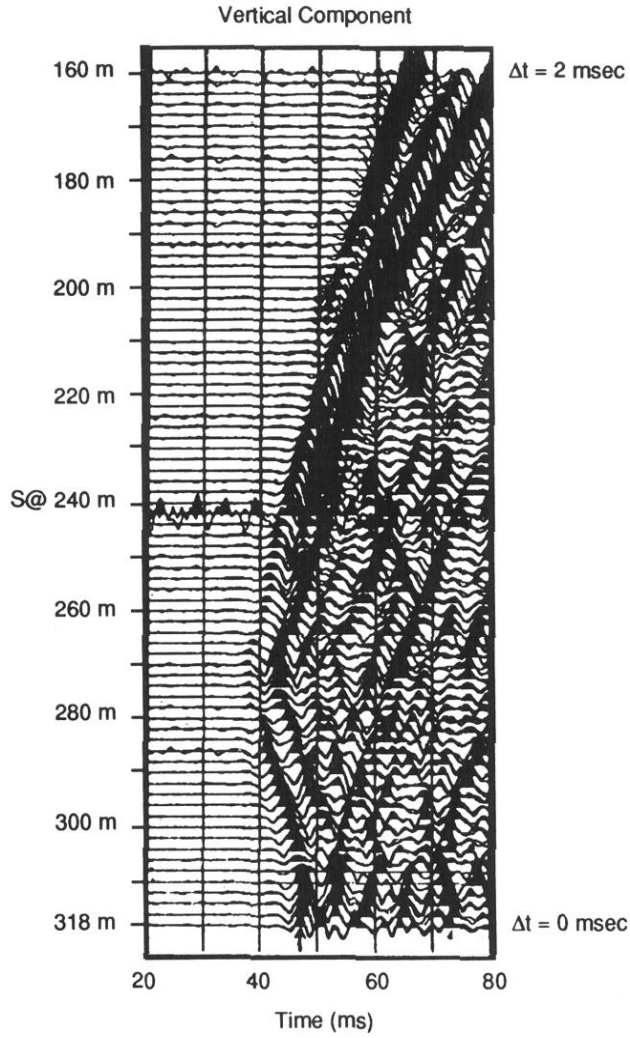

Figure 6. Overlay of traces from survey 1 and 2 as recorded on the Ch4-Ch2, 240-m common source fan. Overlay is very good below about 250 m, giving a measure of survey repeatability.

tion to enhance the direct arrival and also to discriminate between shear waves and S-to-P converted waves on the basis of particle motion. Results were not as good as expected, probably because in the difficult data zones, where we needed improvement, there was nonlinear particle motion due to overlapping arrivals of P and/or S waves.)

The traveltimes were then put into a tomography inversion program (described by Aldridge and Oldenberg in Vol. 2 of the *Journal of Seismic Exploration*, 1993). An important feature of this program is stabilizing constraints. Tomography inversion is nonunique and unstable unless the target is surrounded by sources and receivers, something which is possible for medical tomography but not for crosswell tomography. Thus we must supplement the data by mathematically imposed constraints, usually smoothing. Unfortunately, smoothing results in a loss of resolution.

We think a better technique is to use a reference model determined from sonic logs. This brings in outside knowledge and preserves the high frequency character of the velocity distribution. In the tomogram discussed in the next section,

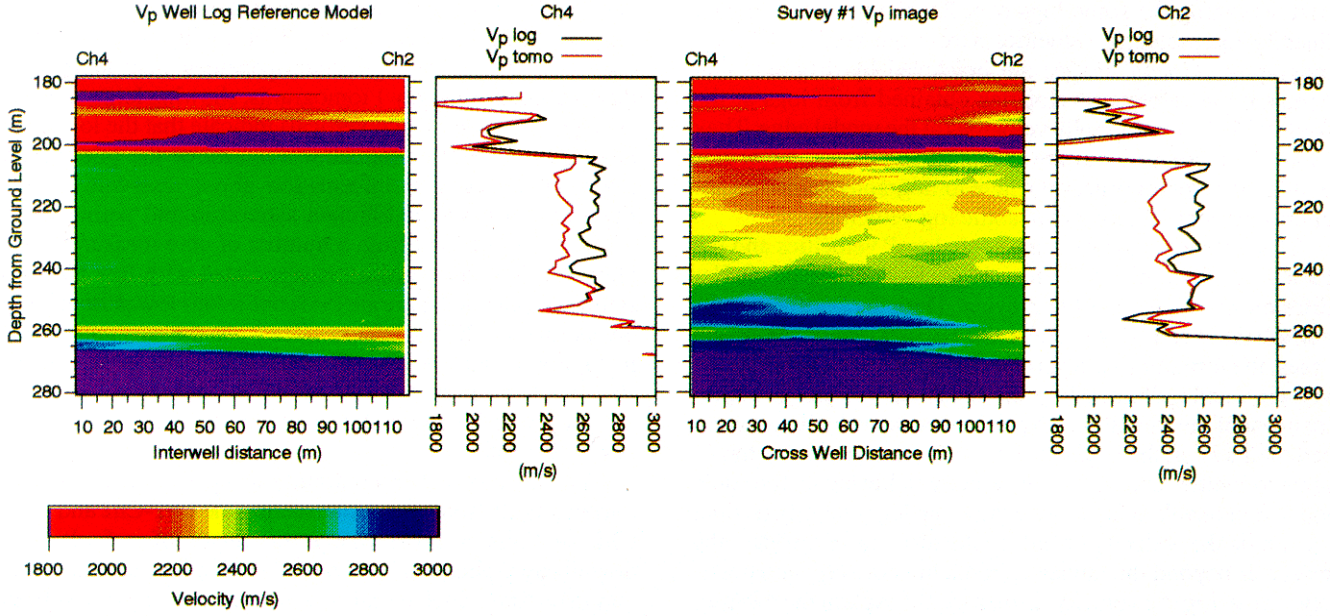

Figure 7. P-wave reference model (left). Velocity section (right) is the P-wave velocity tomogram from the first survey in Ch4Ch2. Traces on either side of the tomogram show sonic log velocities in black and tomogram velocities at the model edge in red.

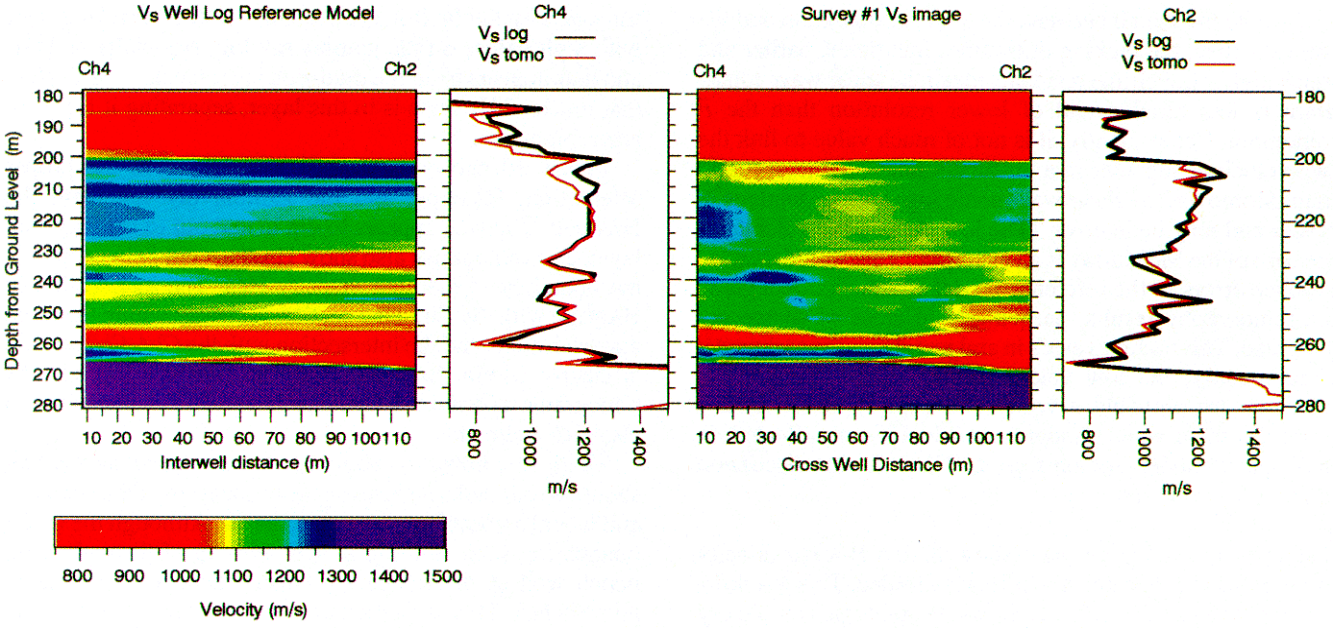

Figure 8. S-wave velocity tomogram from the first survey in Ch4Ch2. Tomogram and log velocities agree much better for shear waves than for P-waves. Shear traveltime picks below 260 m are questionable and sparse; consequently, the tomogram velocities below about 250 m are heavily influenced by the reference model.

the velocities that cannot be resolved by the observed traveltimes retain the values of the reference model. Thin layers in the model (i.e., below the resolving power of the tomography) will cross over to the final model if the velocities of these layers are consistent with the traveltime picks of seismic data in the region. We feel this is valid because the model is based on data from logs. In our opinion, we are combining knowledge in a consistent way.

Velocities distribution from tomography. Figures 7-8 show P and S wave tomography velocities from the first survey at Ch4-Ch2. The reference models were computed by first averaging the sonic logs over 2.0-m intervals and then linearly interpolating velocities across the section. The tomography velocity images are bracketed by diagrams that compare the reference velocities obtained from logs at the wells with the tomography velocities at the model edge. They should be close, and they are except for the P-wave velocities within the reservoir interval where tomography velocities are almost 10 percent lower than sonic log velocities.

The difference between the sonic log *P* velocities and the tomogram *P* velocities is curious. We have observed similar differences in crosswell surveys at Duri, Indonesia, an unconsolidated sandstone, and Lost Hills, a diatomite. In all cases, the formations are porous and exhibit very low P-wave velocity, and quite possibly the mudcake velocity is higher than that of the formation. Typical mudcake velocity for these sediments is on the order of 2600 m/s which is above tomogram velocities and about the velocity indicated by the sonic log at Steepbank. It is possible the sonic log is simply reading the mudcake velocity. Mud could also have invaded the reservoir beyond the mudcake, reducing porosity, and possibly increasing the velocity. Either would explain the discrepancy. Note that the S-wave tomogram and log velocities agree fairly well, which is expected since mud invading the formation pore space would not increase shear velocity much due to the added density of the rock which would offset any increase in the shear rigidity.

Despite the match between the S-wave tomogram and the log velocities, the picking difficulties mentioned earlier and much higher traveltime residuals mean the shear wave tomogram is less reliable and of lower resolution than the *P* tomogram. Consequently, it is not of much value to link the two velocities together in a Poisson's ratio or velocity ratio map. Moreover, the shear wave sonic logs look anomalous in places and may be in error. (The low shear wave velocity at the base of the McMurray is an example.) This would, in turn, produce errors in the reference model which would degrade the tomography results, particularly in areas of sparse ray coverage. This includes areas in and just above the carbonate. Consequently, the low velocity zones at the base of the reservoir are probably a vestige of a questionable model. Since the shear wave tomography velocities are affected by picking and model problems, we will limit further discussion to P-wave velocities.

Interpretation. Figures 9a-b show all four P-wave velocity tomograms attached end-to-end and unfolded. This is a difficult way to view them, but it shows the geologic complexity within the volume of the investigation and the good match at the tomogram edges. The effect of steam injection is clearly seen by the increase in red colors, signifying reduced velocity, in the figure (9b) from the second survey. Large velocity changes, however, appear only on the Ch4-Ch2 section. Comparing the distribution of the red colors with the location of the HAsPipe and the steam injector (IN1) indicates the heat has not followed the expected path along the HAsPipe. Instead, it has migrated upward around the injector, encountered several zones of high permeability, and headed off toward Ch4.

The tomograms also provide new information on reservoir definition. Superimposed are the gamma ray and resistivity logs from several observation wells. Also shown in Figures 9a,b is the well log-based geologic model. The low velocity gas cap (purple) and the high velocity carbonate (blue) stand out clearly on all sections. The tar sand lies at 205-260 m. Despite a large number of excellent quality well logs, few lateral or vertical geologic heterogeneities were mapped in the tar sand. The survey 1 tomograms, showing large velocity changes (both lateral and vertical) indicate that the log based model, used for the production forecast of the pilot steam flood, lacks essential information about reservoir details. Figure 9a also shows bitumen saturation and permeability which were obtained from a number of core measurements. Note that low permeability is associated with low bitumen saturation, and that there are two continuous low permeability layers (about 230 and 250 m). They are the two mud layers in Figure 1 and are labeled MD1 and MD2 in Figure 9a. Because low bitumen zones cannot support banking of the tar, they will be routes for steam to escape, which is the observed result.

The sharp lateral discontinuity at approximately 260 m (striking north-south) and intersecting the Chl-Ch2 and Ch4-Ch2 sections is most likely the result of a fault. The downthrown direction is toward Ch2; displacement is a little less than 10 m. Such a fault was tentatively recognized from the log data by a thickening in the lower reservoir at Ch2. The four tomograms give a more complete view of the complexity of the geology around the fault.

A high velocity lens, about 245-250 m, is present on all tomograms except Ch4-Ch3. It is discontinuous and appears truncated by the fault in section Chl-Ch2. It correlates well with high values on the gamma ray log, especially at TO1, and thus appears to be the mud-rich layer labeled MD2. Note that much of HAsPipe is in this layer, separating it from the reservoir above.

Figure 10 shows the tomograms folded in the proper orientation, HAsPipe, and the gamma ray log from the HASWell. The well appears to dip in and out of the clay-rich layer. The tomograms also show HAsPipe either in or right at the boundary of the high velocity lens. The intersection of HAsPipe with the Chl-Ch2 section is clearly within the more clay-rich zone, and the intersection with the Ch4-Ch3 section is clearly within the sand. Both the HAsPipe log and the tomograms indicate that HASPipe is either in or very close to clay-rich sediments.

There are, however, some tomogram discrepancies that should be pointed out since they are a measure of the accuracy and lateral smoothing of the tomograms. Although the major boundaries, such as the gas layer and top of the carbonate, match well at the tomogram edges, there are some layer mismatches. This is particularly true at the Ch4-Ch2/Ch1-Ch2 and Ch4-Ch2/Ch4-Ch3 intersections. They may be partly due to lateral discontinuity of reservoir sediments and lateral smoothing. The tomograms strike off in different directions, and thus the velocities at the edges are influenced

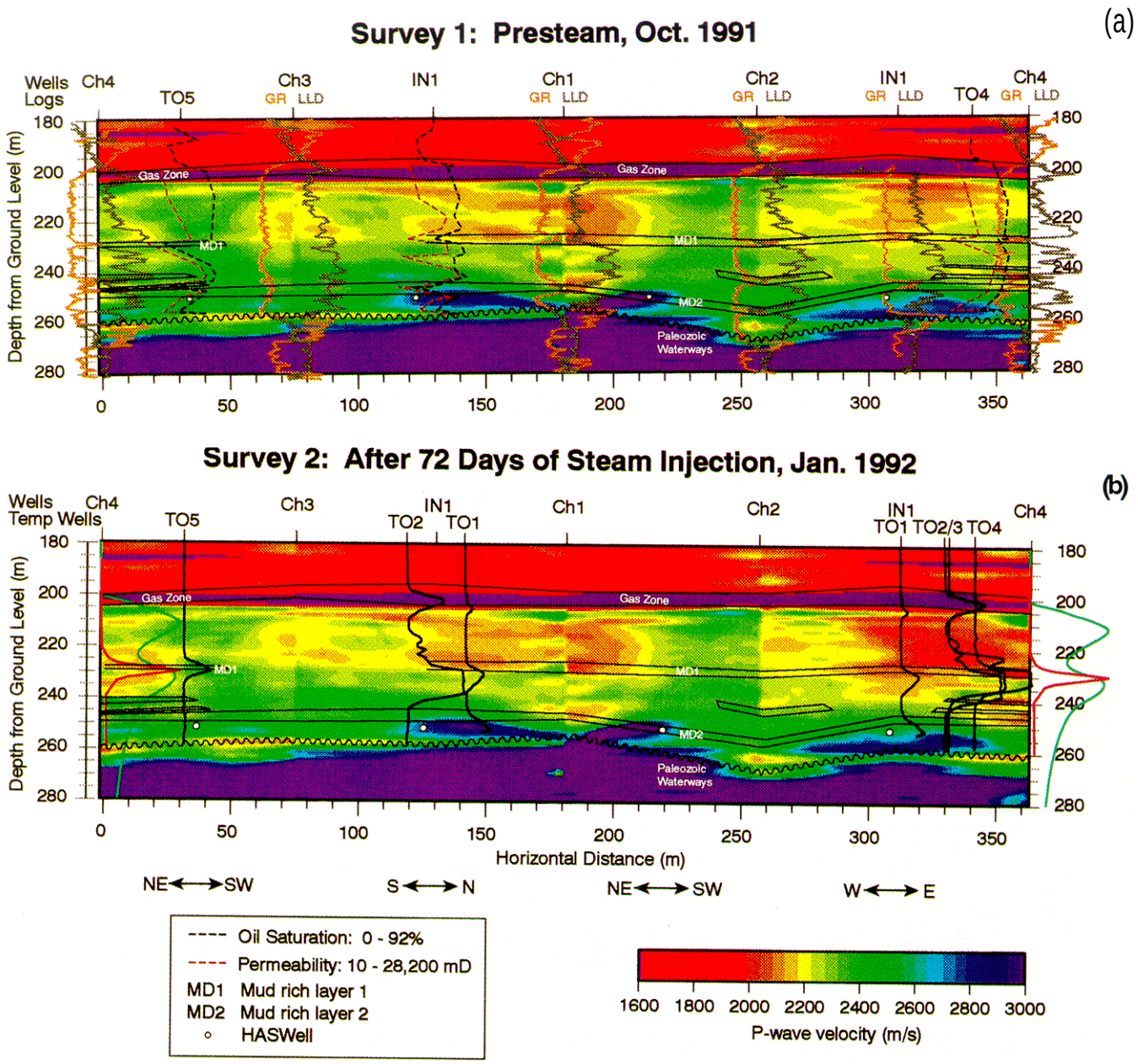

Figure 9. Four P-wave velocity tomograms. Overlayed on (a) are gamma and resistivity logs from indicated wells; bitumen saturation and permeability from core measurements in T05, IN1, and T04; and the geologic model. In (b) the decrease in P-wave velocity, indicated by an increase in the red colors in section CH4CH2, shows the direction taken by the steam. The steam, injected near the center of the figure at about 250 m, appears to have risen about 20 m around the wellbore and then escaped to the east. Also shown are temperature logs from several wells. Two are shown for CH4. The one with the single spike was taken at the time of the second crosswell survey; the other, taken six weeks later, shows how the heat has expanded upward, which is also apparent on the tomogram. Relative direction from the injection well and/or the HASPipe along each profile is shown below (b).

by smoothing across different regions. Also note that at IN1 where the tomograms Ch4-Ch2 and Chl-Ch3 intersect, the depth of the high velocity lens is about 5 m lower on Ch4-Ch2 than on Chl-Ch3. The latter agrees with the IN1 gamma ray log, so Ch4-Ch2 is reading low. This discrepancy may be due to the fault mentioned earlier: Ch4-Ch2 is smoothing across the fault, whereas Chl-Ch3 is entirely on the upthrown side.

Velocity change and temperature measurements. At present crosswell seismology is still an emerging technology, and few engineers would trade a temperature observation well for a crosswell survey for steamflood monitoring. A well can provide continuous temperature measurements in time and depth, and there is no ambiguity in interpreting temperature change from velocity change. On the other hand, crosswell tomography can detect heat migration in two (and potentially three) dimensions, and improve reservoir definition which could be important when problems are encountered in the drive. Even when a crosswell survey is run, information from temperature observation wells helps interpretation of tomography velocities. The relationship between temperature increase and velocity reduction is complex because many

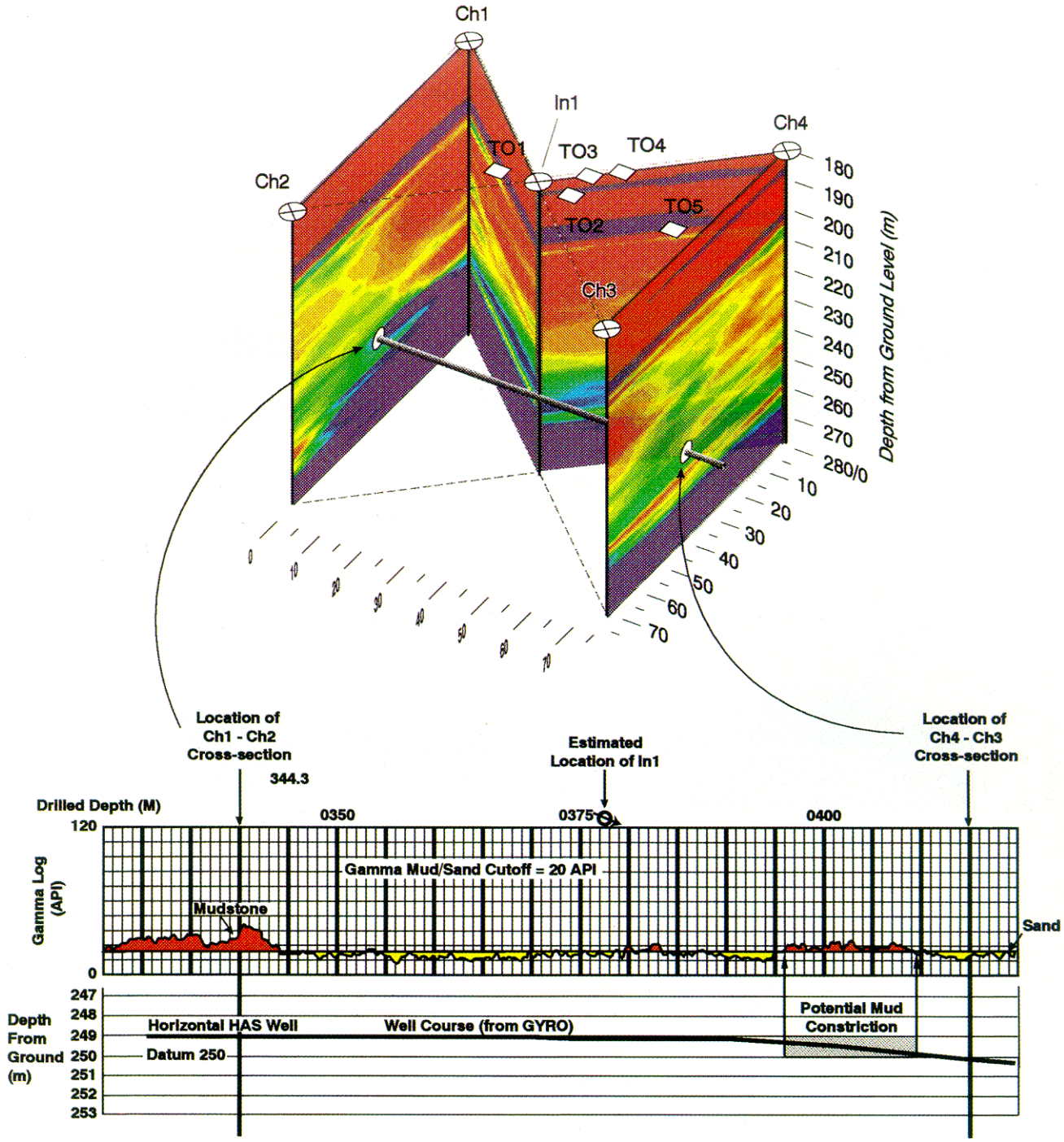

Figure 10.3-D view of the combined tomograms (top). Gamma ray log, course of the HASPipe, and geologic information (bottom). High gamma values at Chl-Ch2 correlate with the high velocity area seen in tomographic section. Low gamma values in the HASPipe log at Ch4Ch3 correlate with low velocities indicating sand in this section at the depth of the HASPipe.

variables (oil gravity, oil saturation, porosity, etc.) affect it.

Figure 11 illustrates the effect of bitumen saturation. Three samples of different saturation were heated from 20 to 125" C, and the resulting decreases in P and S wave velocities were plotted against the saturation. The P-wave velocity reduction changes from 28 to 5 percent as saturation decreases (and is replaced by formation water) from 80 to 20 percent. Clearly, when saturation changes as steam passes through a reservoir, velocity reduction can only give a qualitative picture of the heat movement, not an estimate of the actual temperature. As seen in Figure 9a, bitumen saturation varies considerably within the reservoir and this will cause varying velocity responses to temperature changes.

First note that temperatures at TO1 (Figure 9b), very close to the injection well, register a very small increase at 230 m, the depth of MD1. On the other hand, to the east of the injection well, temperatures in the 230-m layer have risen substantially at wells T02, T03, and TO4-the layer probably contains steam. Figure 9b shows heat has reached all the way to Ch4. At T05, to the southeast, there is a temperature increase in the 230-m layer, but it is lower than that observed to the east. Thus the steam is heading east toward Ch4 along

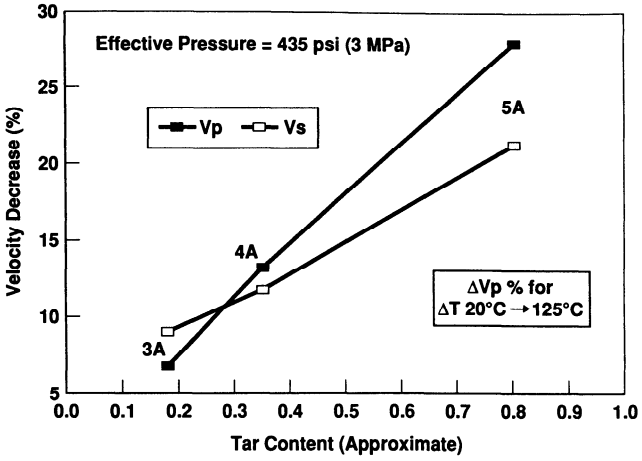

Figure 11. Plot of velocity decrease for 105° C increase in temperature for three core samples of different bitumen saturation. Velocity is very sensitive to temperature change only for rocks with high bitumen content.

a broad front. (It is probably also moving northeast, but there are no observation points in that direction.) A second hot zone is seen in the TO3 well at about 200 m; it is the gas cap at the top of the reservoir. A few weeks later, this hot zone also reached well TO4.

Tomography shows the major velocity change on the east half of Ch4-Ch2 is consistent with well temperatures. There is very little difference in the Chl-Ch3 velocities, suggesting heat is not moving north-south. There is no velocity difference in Chl-Ch2, which is expected from the weak temperature response in TO1, which lies in the path to the section. Finally there is a velocity decrease in the northeast portion of Ch4-Ch3, but it is much less than that seen on Ch4-Ch2. In fact, the boundary between the sections does not fit well within the heated zone, suggesting more heat along Ch4-Ch2 than along Ch4-Ch3. The tomograms do provide information of velocity changes/steam movement in areas where there are no temperature wells. This shows that crosswell seismic surveys cover a larger volume than the five temperature observation wells.

Figure 13 combines the available information into a map view of heat distribution. It appears that the steam, injected at 250 m, rose within the annulus between the casing and the formation and escaped eastward, first through a zone containing the mud layers of low bitumen saturation at about 230 m, and then through the gas cap at about 200 m.

We can only speculate on the reasons for steam movement. Any permeable layer of low bitumen saturation, such as the gas cap, would act as a thief zone since there would be no tar banking. The low saturation, measured on the mud-rich sample at 230 m, may extend upward into the high-permeable sandstone also creating a thief zone. Perhaps compaction and dewatering of the mud, if they occurred after oil migration, created a layer of low bitumen saturation within the sand.

The eastward motion of the steam may be related to the stratigraphic framework and the presence of the (sealing?) fault to the west of IN1. A close look at the heat distribution shows it to be similar to the patterns of velocity variation within the reservoir. For example, the velocity reduction seen in Ch4-Ch2 occurs within a region that already exhibits lower than average reservoir velocity. Also the heat pattern roughly follows the trend of the high-velocity, mud-rich lens dis-

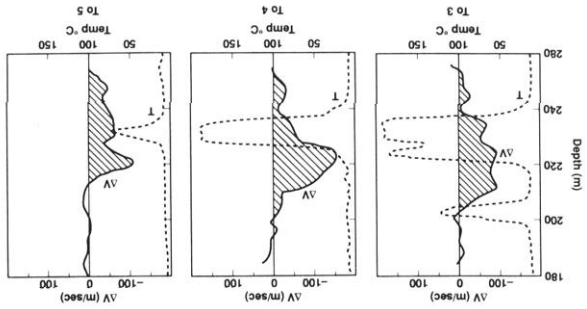

Figure 12. Temperature in various observation wells at time of survey 2 and tomogram velocity reduction seen at location closest to each well. Correlation appears only fair due to rapid lateral variation in temperature, smoothing inherent in fhe tomograms, and large variations in bitumen saturation. High temperature at 200 m is in the reservoir gas cap and would not affect velocity since P-wave velocity in water or gas saturated rock changes very little with changes in temperature.

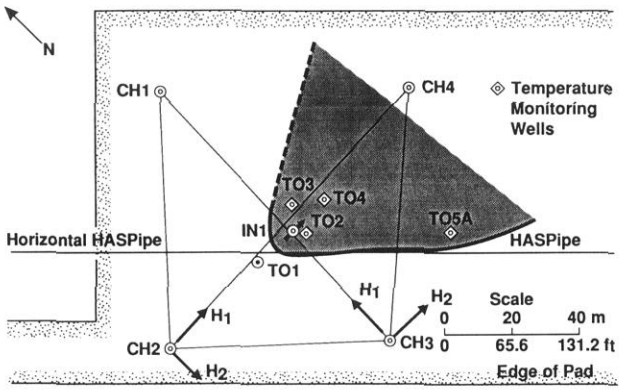

Figure 13. Map view of the approximate heat pattern at the time of survey 2. Well locations are at TD as compared with Figure 1 which shows surface locations.

cussed earlier. This agreement is only fair, however. The mud-rich lens, as well as the low velocity sediments that trap heat in Ch4-Ch2, are seen on Chl-Ch3, and there is no apparent heat in this direction--although it could be very close, there. are no data to suggest otherwise.

Figure 12 shows temperature surveys taken at the time of the second crosswell survey along with the tomogram velocity differences extracted from the location closest to the corresponding observation well. The correlation between the two curves is only fair. In reviewing the velocity reduction and the temperature increase, we note that the former is smeared out over a depth interval much larger than the high temperature zones, and the maximum velocity decrease is about 5 m higher than the maximum temperature. Moreover, no velocity reduction corresponds to the temperature increase in the gas cap, which is expected since the P-wave velocity

is already low due to gas. Furthermore, the P-wave velocities are insensitive to temperature changes in water or gas sands. The correlation is thus a measure of both the resolution of tomography inversion and the complexity of the velocity-temperature relationship.

Comparing temperatures in TO3 and TO4 indicates that the thickness of the heated zone is growing upward. These zones have higher bitumen saturation, so the resulting velocity reduction will be much greater than in the low bitumen, high water-saturated, but hotter zone below. Lateral smearing would show the tomogram velocity reduction beyond the boundaries of the high temperature bank. This implies that the lateral smoothing would have to be at approximately 10 m, consistent with the smearing discussed earlier in connection with the tomogram edges and the high-velocity muddy layer at 250 m.

Summary and conclusions. At Steepbank tomography does a good job of defining geology and detecting movement of heat. We estimate the lateral resolution of the heat distribution map to be approximately 10 m. Moreover, the velocity-temperature relationship is dependent on many factors, among them bitumen saturation and the presence of gas, so velocity reduction cannot be used to estimate actual temperatures without other constraints. The resolution and accuracy of the tomograms depend on geology and raypath distribution, both very complex at Steepbank. To increase the resolution of crosswell seismology, we need to combine tomographic velocity imaging using the first arrivals with imaging of the reflected events seen in Figures 4-5.

The tomography also provided new information about the reservoir. The configuration of the high velocity, clay-rich lens and its proximity to HAsPipe was unknown beforehand, and the existence of a fault was only suspected. The variations and trend of the tomogram velocity distribution suggest the reservoir is complex, and in fact the trend appears to control the heat movement.

It is important to assess if the tomograms would have had a significant influence on the HASDrive project if available beforehand. Most likely HASPipe would have been drilled a bit shallower to avoid the high velocity, mud-rich lens. More attention may also have been paid to the gas cap and other reservoir heterogeneities. This may have led to a more realistic geologic model for the flow simulations and perhaps greater caution in the detailed design of the project.

The tomograms, however, do not have the resolution to directly build a flow model, nor is there a simple relationship between the velocity and the relevant flow parameters.. An interesting continuation of this work would use the tomograms to estimate the horizontal variogram in a statistical model. These variograms could then be used to estimate porosity or oil saturation distribution for input to reservoir simulation.

The data have been given to universities for further research, so we can expect to hear more about them.

Acknowledgements: We would like to express our appreciation to Chevron Petroleum Technology Companyfor approving this project and for allowing publication of the results. Al Cogley is acknowledgedfor his contributions to data acquisition. We are also grateful for the contributions by Dave Aldridge during data processing.